

Supplementary information

mRNA engineering for the efficient chaperone-mediated co-translational folding of recombinant proteins in *Escherichia coli*

Le Minh Bui^{1,2,†}, **Almando Geraldi**^{3,†}, **Thi Thuy Nguyen**³, **Jun Hyoung Lee**¹, **Ju Young Lee**⁴, **Byung-Kwan Cho**^{1,3,5,*} and **Sun Chang Kim**^{1,3,5,*}

¹ KAIST Institute for BioCentury, Korea Advanced Institute of Science and Technology (KAIST), Daejeon 34141, South Korea; junhlee@kaist.ac.kr (J.H.L.)

² NTT Hi-Tech Institute, Nguyen Tat Thanh University (NTTU), Ho Chi Minh City 700000, Vietnam; blminh@ntt.edu.vn (L.M.B.)

³ Department of Biological Sciences, Korea Advanced Institute of Science and Technology (KAIST), Daejeon 34141, South Korea; almandogeraldi@kaist.ac.kr (A.G.); nguyenthuy@kaist.ac.kr (T.T.N.)

⁴ Center for Bio-based Chemistry, Korea Research Institute of Chemical Technology (KRICT), Ulsan, 44429, South Korea; juylee@krict.re.kr (J.Y.L.)

⁵ Intelligent Synthetic Biology Center, Korea Advanced Institute of Science and Technology (KAIST), Daejeon 34141, South Korea

* Correspondence: sunkim@kaist.ac.kr (S.C.K.), bcho@kaist.ac.kr (B.-K.C.); Tel.: +82-42-350-2619 (S.C.K.); Tel: +82-42-350-2620 (B.-K.C.)

† These co-first authors contributed equally to this work.

BMP2NdeF	TGATAACATATGCAAGCCAAACACAAACAG
TliANdeF	TGATAACATATGCATCATCATCATCATCATCACAGCA
TliAEcoR	CTGAGAATTCTCATCATTAACTGATCAGCACACCCTCGCTCC
TliAFPoI	GTTTTTIGACGACCTGACCCGCGAGGAGGTGGAATAATGCATCATCATCATCATCA TCATCACAGCA
TliAEcoR	CTGAGAATTCTCATCATTAACTGATCAGCACACCCTCGCTCC
DnaJTliAFPoI	GGAGCGAGGGTGTGCTGATCAGTGAGGAGGTGGAATAATGGCTAAGCAAGATTATTAC G
DnaJEcoR	CTGAGAATTCTTATTAGCGGGTCAGGTCGTCAA
TliA1EcoR	CCGTTAGAATTCTCATCATTAGTCGGTGGTTCGACTCGTG
TliA1FPoI	AGTTTTTIGACGACCTGACCCGCACCGGAGGTACATAATGCATCATCATCATCATC ATCATCACAGCA
TliA1EcoR	CCGTTAGAATTCTCATCATTAGTCGGTGGTTCGACTCGTG
TliA2NdeF	TGATAACATATGAACATCGTCAGCTTCAACG
AdhNdeF	TGATAACATATGTCTATCCCAGAAACTCAAAA
DnaKNcoF	TGATAACCATGGAAGGTAATAAATTGGTATCGACCTGG
DnaKBamHR	CGATTAGGATCCTCATTATTATTTTTGTCTTTGACTTCTTCAAATTC
GrpENdeF	AGCTGACATATGAGTAGTAAAGAACAGAAAACGCC
GrpEXhoR	CGATTACTCGAGTCATTATTAAGCTTTTGCTTTCGCTACAG

Supplementary Table S3. Predicted DnaK binding sequences. The predicted DnaK binding sequences were analyzed using Limbo algorithm with the best overall prediction option and threshold score of 11.08.

POI	Binding area	Binding motif	Score
ScFv (249 aa, 2 disulfide bonds)	35-41	MNWIRQT	11.3
	77-83	KNTLYLQ	12.2
	79-85	TLYLQMT	16.8
	106-112	DFFDYWG	11.7
	166-172	SNYLAWY	22.8
	181-187	QLLIYYA	19.5
HIV1-Pr (106 aa, 1 disulfide bond)	Not found	Not found	Not found
BR2ScFv (267 aa, 2 disulfide bonds)	10-16	GRLLRRL	12.3
	11-17	RLLRRL	12.3
	12-18	LLRRLR	12.7
	13-19	LRRLRG	12.3
	54-60	MNWIRQT	11.3
	96-102	KNTLYLQ	12.2
	98-104	TLYLQMT	16.8
	125-131	DFFDYWG	11.7
	184-190	SNYLAWY	22.8
	199-205	QLLIYYA	19.5
UGD (394 aa, no disulfide bond)	16-22	GLLIAQN	12.7
	75-81	DYVIIAT	11.2
	258-264	TKQLLAN	12.6

	300-306	GIYRLIM	11.9
	301-307	IYRLIMK	13.5
	302-308	YRLIMKS	16
Adh1p (354 aa, no disulfide bond)	33-39	ELLINVK	13
	78-84	ENVKGWK	13.9
	217-223	EVFIDFT	13.5
	257-263	TRYVRAN	12.5
UbiC (208 aa, no disulfide bond)	22-28	TFLRYNA	12.4
	63-69	LDWLLLE	11.7
	65-71	WLLEDS	13.9
	110-116	RYWLREI	11.1
	153-159	GRYLFTS	14.7
	189-195	LLTELF	13.1
	193-199	ELFPAS	15.5
Leptin (152 aa, 1 disulfide bond)	14-20	IKTIVTR	11.3
	16-22	TIVTRIN	11.2
	63-69	QILTSMF	11.9
	95-101	SCHLPWA	12.4
BMP2 (121 aa, 3 disulfide bond)	90-96	MLYLDEN	11.3
	97-103	EKVVLKN	11.5
	98-104	KVVLKNY	11.9
N-terminal sfGFP (217 aa, no disulfide bond)	40-46	GKLTCLKF	12.4
	41-47	KLTLKFI	12.8
	52-58	KLPVPWP	13
	198-204	NHYLSTQ	11.1

Supplementary Figure S1

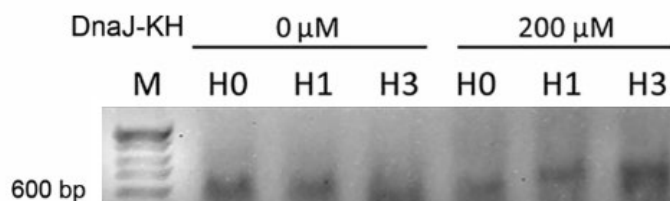


Figure S1. Gel retardation assay to confirm the binding of the DnaJ-KH to the binding hairpins in the CRAS system. Shifted migration of HIV-1 protease mRNA with 1 (H1) and three 3'UTR KH hairpins (H3) observed in the presence of 200 μM purified DnaJ-KH.

Supplementary Figure S2

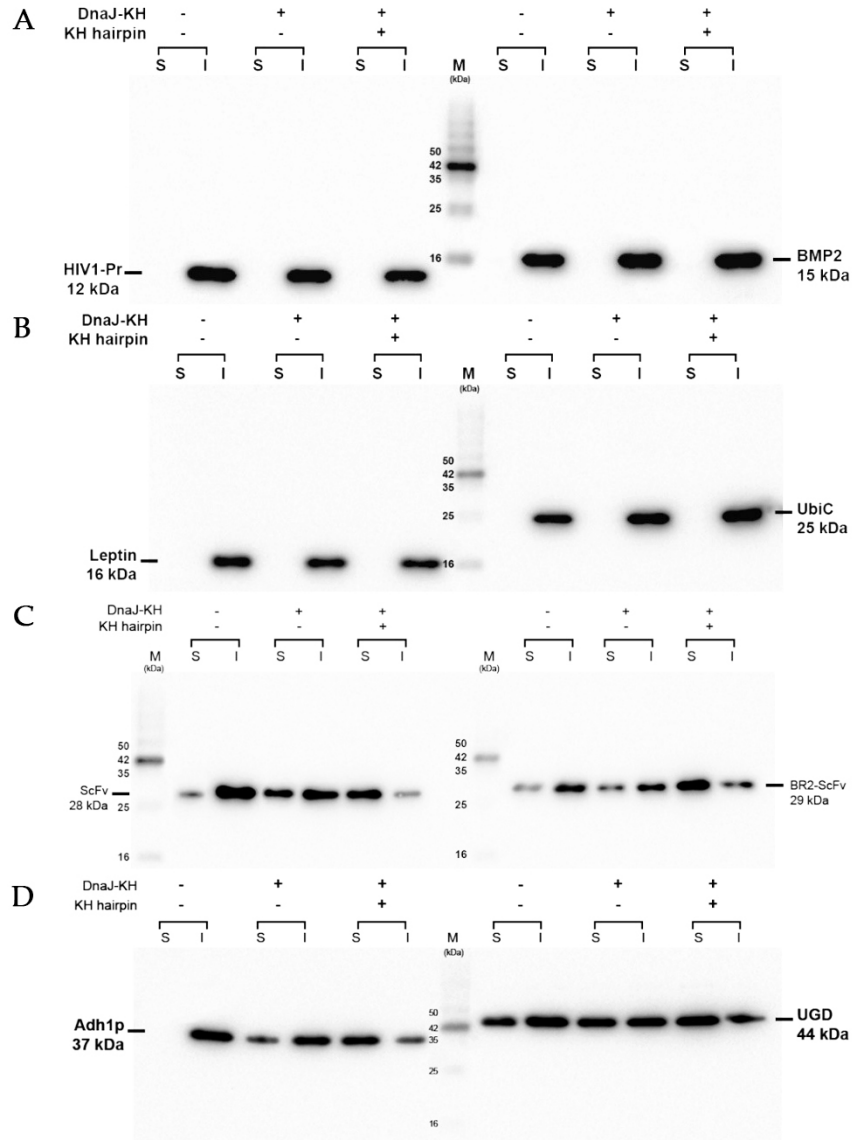


Figure S2. Western Blot analysis of selected recombinant proteins expressed by CRAS system. Lanes S, soluble fraction; Lanes I, insoluble fraction; Lanes M, West-View 10 kDa Western marker (ELPIS Biotech). (A) The expression of HIV1-Pr (left) and BMP2 (right); (B) The expression of Leptin (left) and UbiC (right); (C) The expression of ScFv (left) and BR2-ScFv (right); (D) The expression of Adh1p (left) and UGD (right). Bands corresponding each recombinant proteins are indicated on the sides of the blot. For the evaluation of *in vivo* solubilization effect of CRAS system, the DnaJ-KH without His tag was used.

Supplementary Figure S3

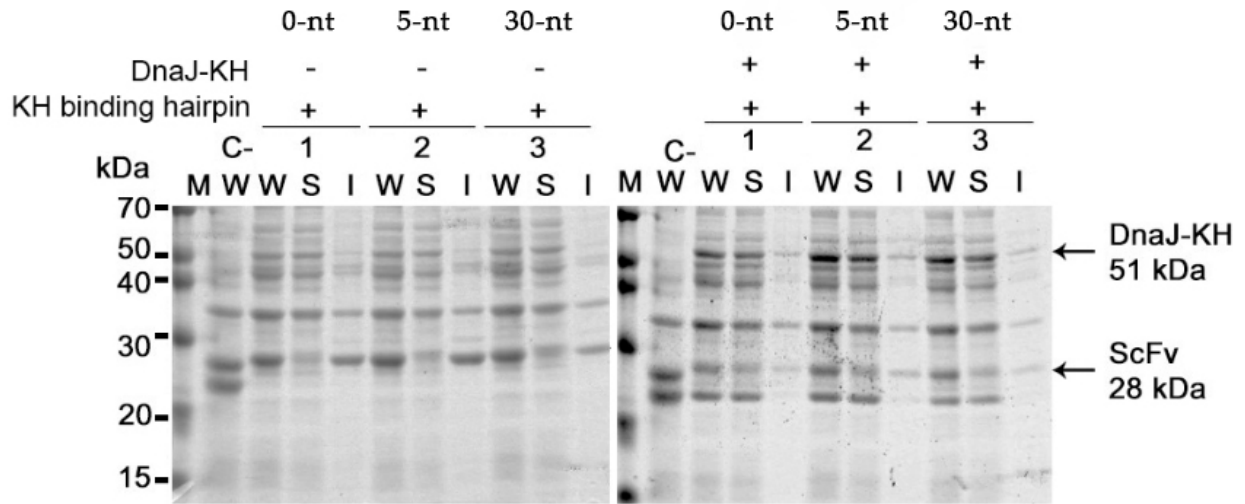


Figure S3. Effect of spacer length between the stop codon and the 3'UTR binding loop on the efficacy of the CRAS system. Coomassie blue stained 10% SDS-PAGE results demonstrating the efficacy of the CRAS system on improving the solubilization of the ScFv in BL21(DE3) strain after 4 h of induction using 0.5 M IPTG. The distance between the stop codon of *scfv* and KH binding loop is indicated on top of each group. Lanes 1, no spacer (0-nt) between the stop codon and 3'UTR binding loop; Lanes 2, in the presence of 5-nt spacer between the stop codon and 3'UTR binding loop; Lanes 3, in the presence of 30-nt spacer between the stop codon and 3'UTR binding loop. Lanes M, Mid-range range pre-stained marker (ELPIS Biotech); Lanes W, whole cell lysate fraction; Lanes S, soluble fraction; Lanes I, insoluble fraction. Bands corresponding to DnaJ-KH (51 kDa) and ScFv (28 kDa) are indicated by arrows.

Supplementary Figure S4

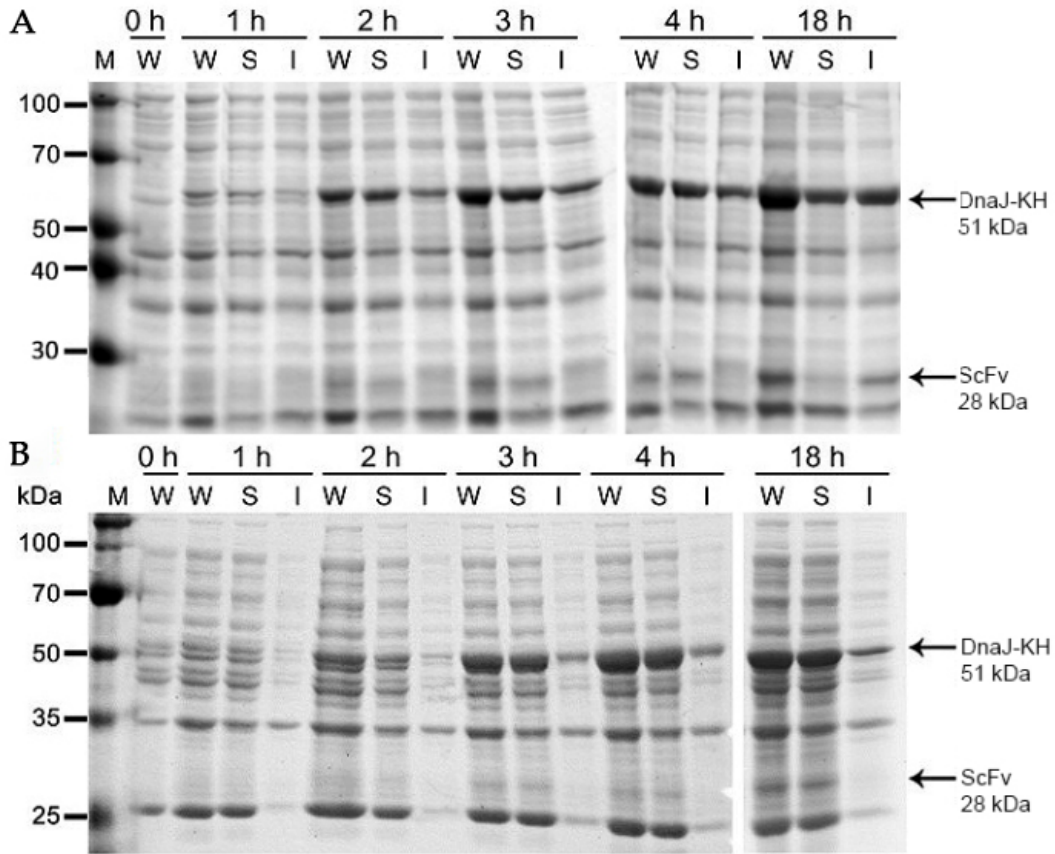


Figure S4. Time course solubilization of ScFv in *E. coli* BL21(DE3). (A) Time course solubilization of ScFv using the CRAS system with 1-loop and (B) 3-loop design; Lane M, Mid-range range pre-stained marker (ELPIS Biotech); Lanes W, whole cell lysate fraction; Lanes S, soluble fraction; Lanes I, insoluble fraction. The time shown on top is the period of cell incubation after the IPTG induction. Bands corresponding to DnaJ-KH (51 kDa) and ScFv (28 kDa) are indicated by arrows.

Supplementary Figure S5

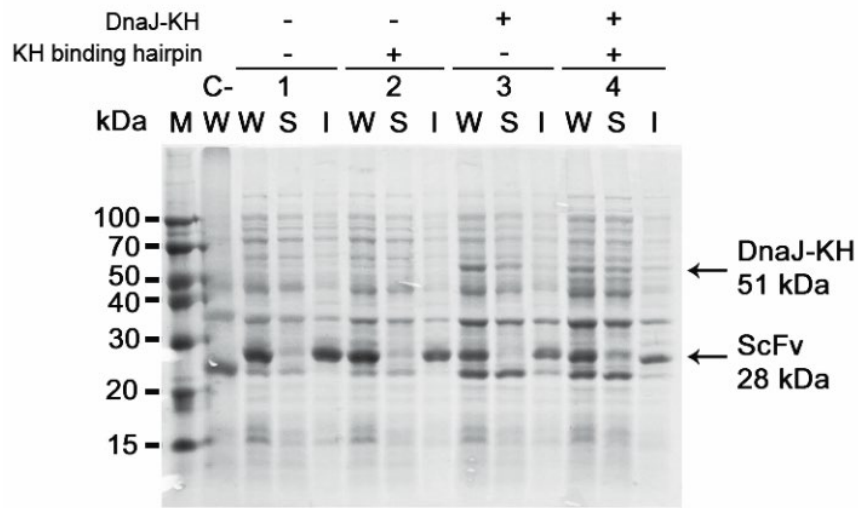


Figure S5. Efficacy of the CRAS system on improving the solubilization of ScFv in the *dnaK* knockout BL21(DE3) strain after 4 h of induction. Lane C-, whole cell lysate of *E. coli* BL21(DE3) harbouring pET16b and pAMT7 (negative control); Lanes 1–4, expression pattern of ScFv in the absence of binding loop and DnaJ-KH (Lanes 1); in the presence of binding loop and the absence of DnaJ-KH (Lanes 2); in the absence of binding loop and the presence of DnaJ-KH (Lanes 3); and in the presence of binding loop and DnaJ-KH (CRAS system) (Lanes 4). Lane M, Mid-range pre-stained marker (ELPIS Biotech); Lanes W, whole cell lysate fraction; Lanes S, soluble fraction; Lanes I, insoluble fraction. Bands corresponding to DnaJ-KH (51 kDa) and ScFv (28 kDa) are indicated by arrows.

Supplementary Figure S6

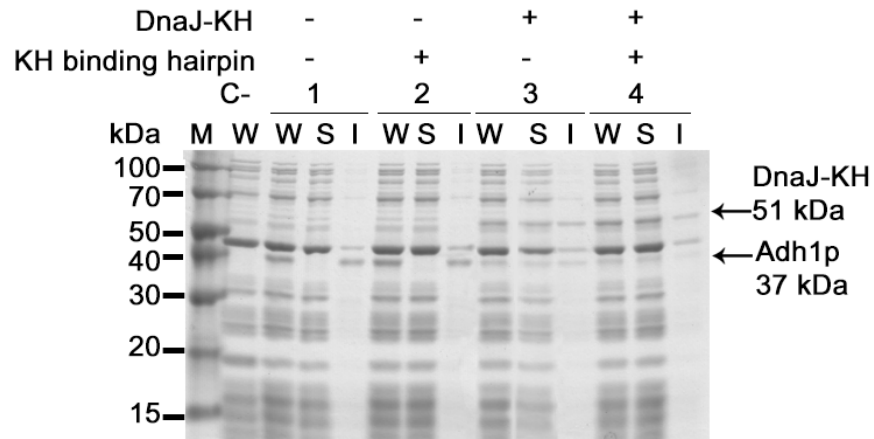


Figure S6. *in vitro* solubilization of Adh1p with DnaJ-KH. pET16b-Adh and pAMT7. Lane (C-); pET16b-Adh and pAMT7 (1); pET16b-Adh3L and pAMT7 (2); pET16b-Adh and pAMT7-DnaJ-KH (3); and pET16b-Adh3L and pAMT7-DnaJ-KH (4) were used as templates for *in vitro* translation using the PURExpress® In Vitro Protein Synthesis Kit. Samples were collected after 4 h of incubation at 37°C and examined by 10% SDS-PAGE.

Supplementary Figure S7

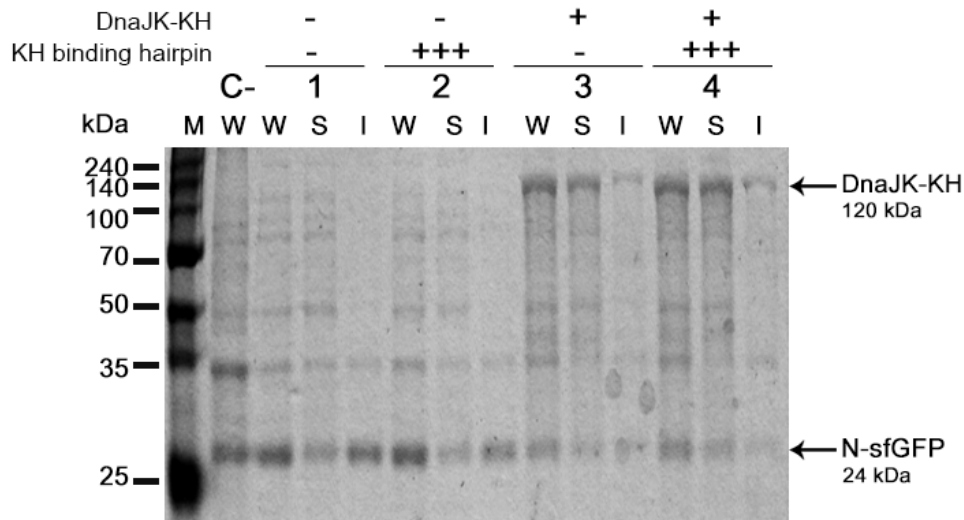


Figure S7. Efficacy of the CRAS system on improving the solubilization of N-terminal GFP (N-sfGFP) in *E. coli* BL21(DE3) after 4 h of induction. Lane C-, whole cell lysate of *E. coli* BL21(DE3) harbouring pET16b and pAMT7 (negative control); Lanes 1–4, expression pattern of N-sfGFP in the absence of binding loop and DnaJK-KH (Lanes 1); in the presence of binding loop and the absence of DnaJK-KH (Lanes 2); in the absence of binding loop and the presence of DnaJK-KH (Lanes 3); and in the presence of 3 repeats of binding loops and DnaJK-KH (CRAS system) (Lanes 4). Lane M, Broad

range pre-stained marker (ELPIS Biotech); Lanes W, whole cell lysate fraction; Lanes S, soluble fraction; Lanes I, insoluble fraction. Bands corresponding to DnaJK-KH (120 kDa), and N-sfGFP (24 kDa) are indicated by arrows. The repeat number of binding loops is indicated by the number of plus symbols.

Supplementary Figure S8

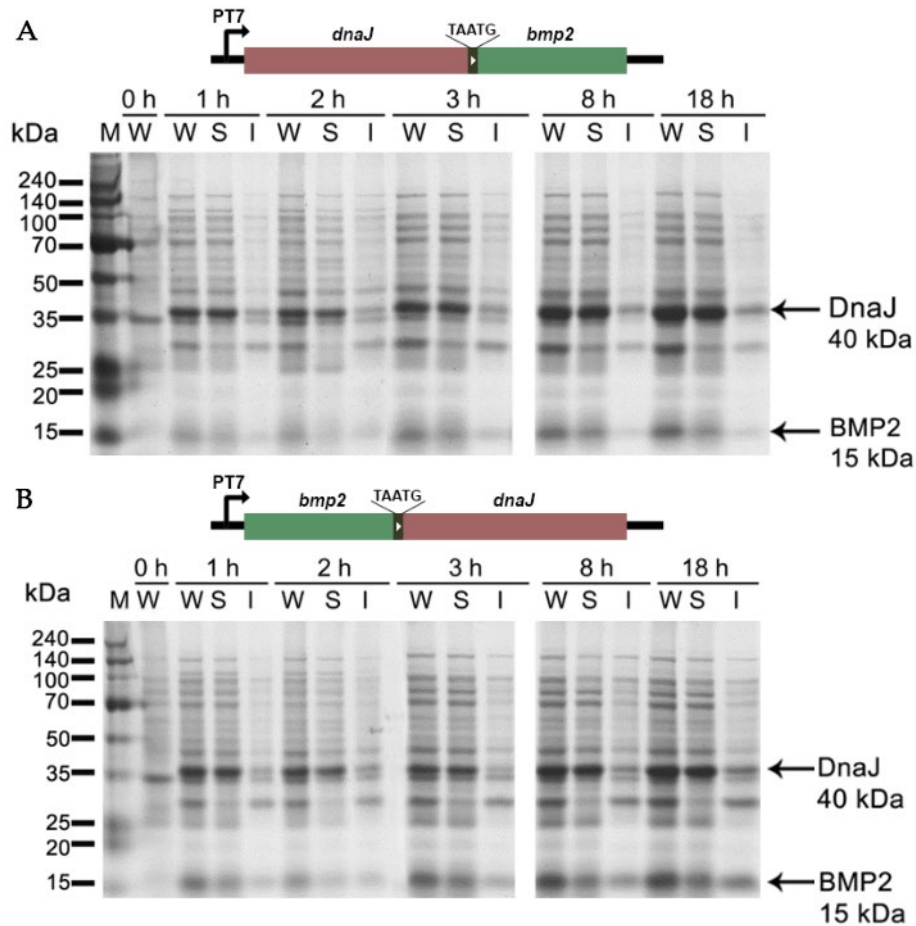


Figure S8. Time course solubilization of BMP2 in the application of the CLEX system. (A) Expression pattern of BMP2 in the CLEX system when placed as the second cistron and DnaJ as the first cistron, and (B) the reverse arrangement. Lane M, Broad range pre-stained marker (ELPIS Biotech); W: Whole cell lysate; S: Soluble fraction; I: Insoluble fraction. Bands corresponding to DnaJ (40 kDa) and BMP2 (15 kDa) are indicated by arrows.

Supplementary Figure S9

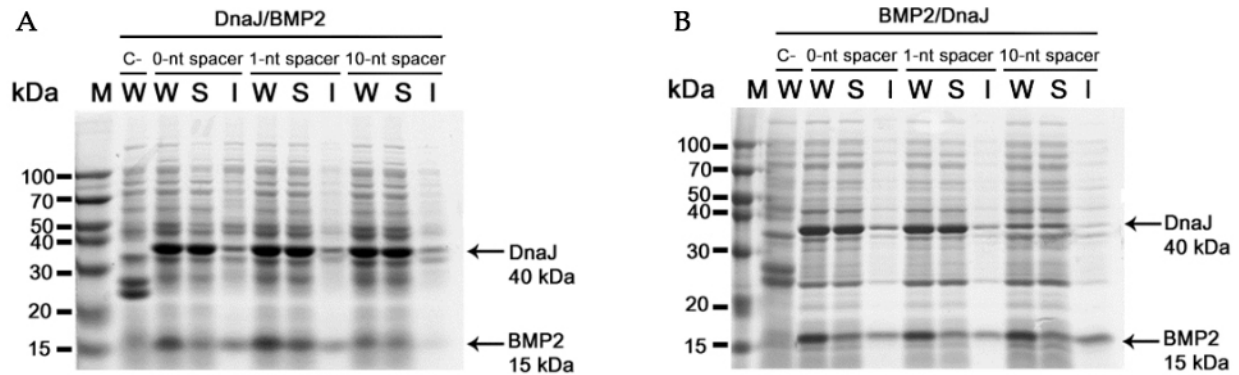


Figure S9. Effect of spacer length between the stop codon of the first cistron and start codon of the second cistron on the efficacy of the CLEX system. Coomassie blue-stained 10% SDS-PAGE demonstrating the efficacy of the CLEX system with 0-, 1-, and 10-nt spacer between (A) stop codon of DnaJ (first cistron) and start codon of BMP2 (second cistron), (B) stop codon of DnaJ (first cistron) and start codon of BMP2 (second cistron) on improving the solubilization of BMP2 in the BL21(DE3) strain after 4 h induction using IPTG. Lane C-, Whole cell lysate of *E. coli* BL21(DE3) harbouring pET16b and pAMT7 (negative control); Lane M, Mid-range pre-stained marker (ELPIS Biotech); W: Whole cell lysate; S: Soluble fraction; I: Insoluble fraction. Bands corresponding to DnaJ (40 kDa) and BMP2 (15 kDa) are indicated by arrows.

Supplementary Figure S10

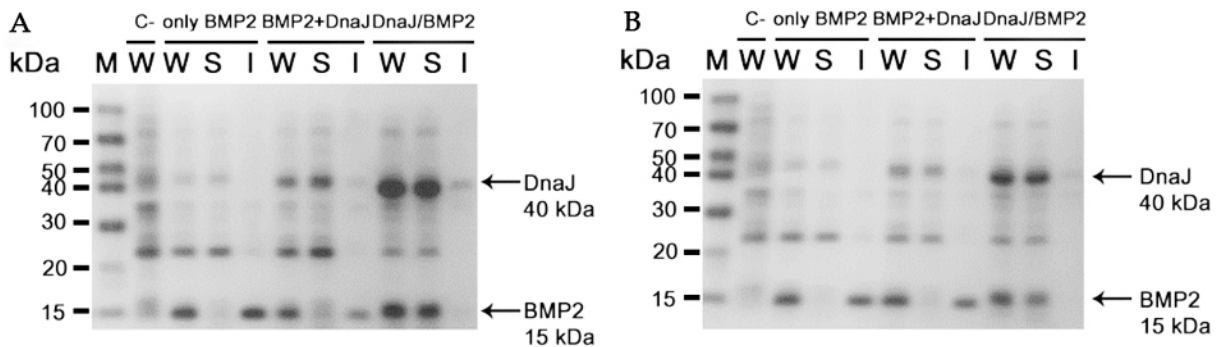


Figure S10. Efficacy of the CLEX system on improving the solubilization of BMP2 in (A) *dnaJ* and (B) *dnaK* knockout BL21(DE3) strain after 4 h of induction. Lane C-, whole cell lysate of *E. coli* BL21(DE3) harbouring pET16b and pAMT7 (negative control); "only BMP2", only BMP2 is overexpressed; "BMP2+DnaJ", BMP2 is co-expressed with DnaJ; "DnaJ/BMP2", BMP2 and DnaJ are expressed in CLEX system when DnaJ as the first cistron and BMP2 as the second cistron. Lane M, Mid-range pre-stained marker (ELPIS Biotech); Lanes W, whole cell lysate fraction; Lanes S, soluble fraction; Lanes I, insoluble fraction. Bands corresponding to DnaJ (40 kDa), and BMP2 (15 kDa) are indicated by arrows.

Supplementary Figure S11

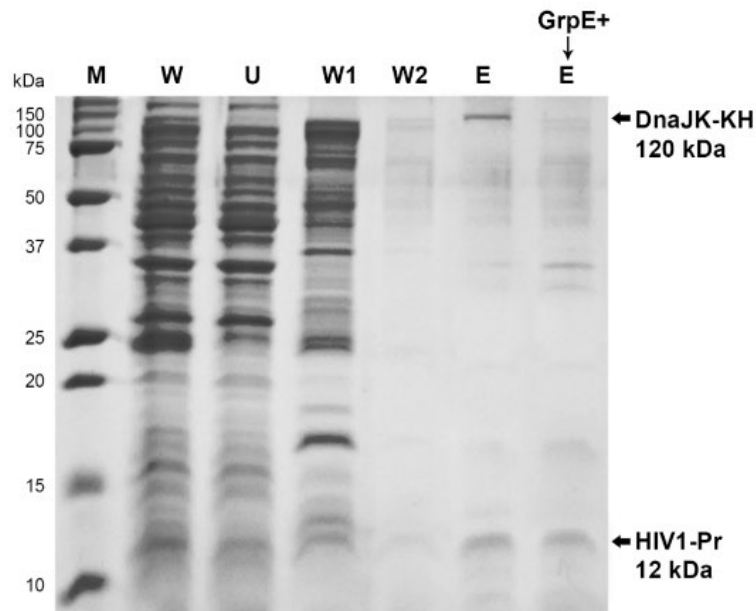


Figure S11. DnaJK-KH is co-purified with HIV-1 protease via Ni-IDA resin. Coomassie blue-stained 10% SDS-PAGE showing the purification of HIV1-Pr (with His tag and 3 × 3'UTR KH binding domains) using the CRAS system. Lane M, Precision Plus Protein Dual Xtra Prestained Standards (Bio-Rad); W: whole cell lysate; U: unbound fraction; W1 and W2: washing fractions using 5 mM and 60 mM imidazole, respectively; E: elution fractions using 500 mM imidazole. The second E lane with the GrpE+ is the elution fraction of the sample co-expressing GrpE with CRAS system. Bands corresponding to DnaJK-KH (120 kDa) and HIV1-Pr (12 kDa) are indicated by arrows.

Supplementary Figure S12

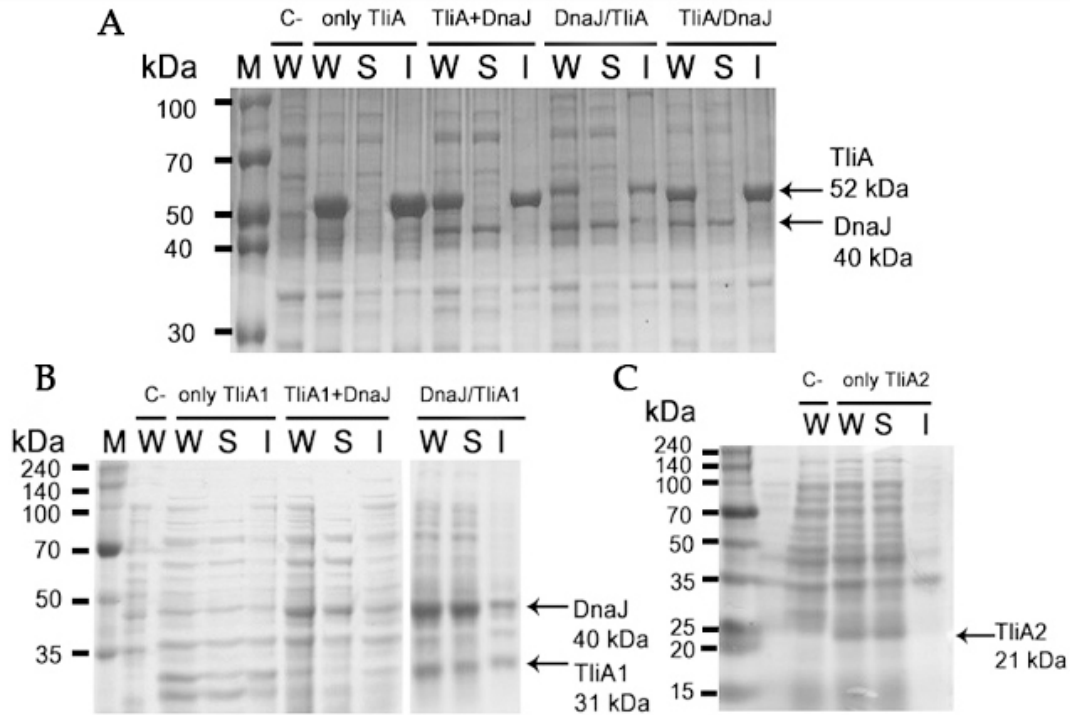


Figure S12. Effect of the CLEX system on the solubilization of (A) TliA lipase (TliA) and (B) TliA fragment containing amino acids 1–300 (TliA1), and the expression pattern of (C) TliA fragment containing amino acids 301–493 (TliA2) in *E. coli* BL21(DE3) after 4 h induction using IPTG. Lane C-, whole cell lysate of *E. coli* BL21(DE3) harbouring pET16b and pAMT7 (negative control); “only TliA, TliA1, or TliA2”, expression pattern of recombinant proteins in the absence of DnaJ; “TliA+DnaJ or TliA1+DnaJ”, expression pattern of recombinant proteins in the presence of DnaJ; “DnaJ/TliA or DnaJ/TliA1”, expression pattern of TliA and TliA1 in the CLEX system when placed as the second cistron, respectively, with DnaJ as the first cistron; “TliA/DnaJ”, DnaJ placed as the second cistron. Lane M, Mid-range or broad range pre-stained marker (ELPIS Biotech); Lanes W, whole cell lysate fraction; Lanes S, soluble fraction; Lanes I, insoluble fraction. Bands corresponding to DnaJ (40 kDa), TliA (52 kDa), TliA1 (31 kDa), and TliA2 (21 kDa) are indicated by arrows.